Editors' Suggestion

Loophole-Free Test of Local Realism via Hardy's Violation

Si-Ran Zhao,[1,2] Shuai Zhao,[3] Hai-Hao Dong,[1,2] Wen-Zhao Liu,[1,2] Jing-Ling Chen,[4,*] Kai Chen,[1,2,5,†] Qiang Zhang,[1,2,5,‡] and Jian-Wei Pan[1,2,5,§]

[1]*Hefei National Research Center for Physical Sciences at the Microscale and School of Physical Sciences, University of Science and Technology of China, Hefei 230026, China*

[2]*CAS Center for Excellence in Quantum Information and Quantum Physics, University of Science and Technology of China, Hefei, 230026, China*

[3]*School of Cyberspace, Hangzhou Dianzi University, Hangzhou 310018, China*

[4]*Theoretical Physics Division, Chern Institute of Mathematics, Nankai University, Tianjin 300071, China*

[5]*Hefei National Laboratory, University of Science and Technology of China, Hefei 230026, China*

(Received 7 January 2024; accepted 9 July 2024; published 7 August 2024)

Bell's theorem states that the quantum mechanical description of physical quantities cannot be fully explained by local realistic theories, laying a solid basis for various quantum information applications. Hardy's paradox is celebrated as the simplest form of Bell's theorem concerning its "All versus Nothing" approach to test local realism. However, due to experimental imperfections, existing tests of Hardy's paradox require additional assumptions of the experimental systems, and these assumptions constitute potential loopholes for faithfully testing local realistic theories. Here, we experimentally demonstrate Hardy's nonlocality through a photonic entanglement source. By achieving a detection efficiency of 82.2%, a quantum state fidelity of 99.10%, and applying high-speed quantum random number generators for the measurement setting switching, the experiment is implemented in a loophole-free manner. During 6 h of running, a strong violation of $P_{\mathrm{Hardy}} = 4.646 \times 10^{-4}$ up to 5 standard deviations is observed with 4.32×10^{9} trials. A null hypothesis test shows that the results can be explained by local realistic theories with an upper bound probability of 10^{-16348}. These testing results provide affirmative evidence against local realism, and establish an advancing benchmark for quantum information applications based on Hardy's paradox.

DOI: 10.1103/PhysRevLett.133.060201

The advent of quantum mechanics has exerted a profound impact on our understanding of the world. While, it is so counterintuitive that there exist severe controversies for quantum theory, such as Einstein-Podolosky-Rosen's argument on the completeness of the quantum description of physical reality [1]. At the heart of Einstein-Podolosky-Rosen's argument lies the paradox between the probabilistic description by quantum theory and the local deterministic description by classical theory of physical reality. In response to this argument, Bell presented an inequality as a test to determine whether quantum behavior could be explained by local hidden variable (LHV) models [2,3]. In quantum theory, the violation of a Bell inequality can be achieved, indicating that the results from quantum theory cannot be fully explained by LHV models [4]. This phenomenon is known as Bell nonlocality [5]. Experimental demonstrations of the Bell nonlocality, along with the routine of Bell inequalities, have been conducted soon after its derivation [6,7], and recently have been pushed into the regime of loophole-free realization [8–14], which promotes a vast range of *device-independent (DI) applications* [15–34].

In addition to Bell inequalities, there exist other approaches to demonstrate nonlocality, such as Bell's theorems without inequalities, which have emerged since the Greenberger-Horne-Zeilinger theorem [5,35,36]. The Greenberger-Horne-Zeilinger theorem pioneers an "All versus Nothing" way to test local realism. However, at the very beginning, it was only applicable to three or more party quantum systems. Soon after, Hardy's paradox was proposed as the "simplest version of Bell's theorem" by simultaneously maintaining the 'All versus Nothing" feature and being applicable to two-party systems [37,38]. Specifically, Hardy's paradox is interpreted as that the conditions $P(00|A_2B_2) = 0$, $P(01|A_1B_2) = 0$, $P(10|A_2B_1) = 0$, must lead to $P(00|A_1B_1) = 0$ for the LHV models. However, it can maximally achieve Hardy's value $P(00|A_1B_1) = [(5\sqrt{5} - 11)/2]$ by quantum theory [37]. Here, $P(ab|xy)$ is the joint probability involving two parties, Alice and Bob, with $x \in \{A_1, A_2\}$ and $y \in \{B_1, B_2\}$ being measurement

*Contact author: chenjl@nankai.edu.cn
†Contact author: kaichen@ustc.edu.cn
‡Contact author: qiangzh@ustc.edu.cn
§Contact author: pan@ustc.edu.cn

inputs and $a, b \in \{0, 1\}$ being measurement outputs for Alice and Bob, respectively [5]. Along with this fundamental interest, Hardy's paradox also finds its applications in quantum information processing, including DI dimension witness, DI quantum randomness certification, DI quantum key distribution, and self-testing of quantum systems [39–44].

Despite great efforts by experimentalists [45–52], a loophole-free Hardy's paradox test is still missing, significantly limiting its related quantum information applications. In this Letter, we challenge local realism with Hardy's violation by utilizing polarization-entangled photon pairs with a high fidelity of up to 99.10%, fast random basis choices, and a high detection efficiency of around 82.2% to obtain the joint probabilities of Alice and Bob. Specifically, by simultaneously closing the *locality loophole* and *detection loophole* and using high-speed quantum random number generators (QRNGs) to guarantee random measurement setting choices, we demonstrate a Hardy's violation of $P_{\text{Hardy}} = 4.646 \times 10^{-4}$ up to more than 5 standard deviations with a set of events containing 4.32×10^9 trials during 6 h of running time (for local realistic theory, the Hardy's value should be $P_{\text{Hardy}} \leq 0$). Through the null hypothesis test following the prediction-based-ratio (PBR) method [53], the upper bound of the probability that local realistic theories can reproduce the observed Hardy's correlation is $p \leq 10^{-16348}$. These results provide strong evidence that quantum mechanical predictions cannot be described by local realistic theories. Moreover, our results serve as a benchmark for quantum information applications based on Hardy's paradoxes.

One of the main obstacles for the loophole-free Hardy's paradox test is that, compared with Bell inequality tests, theoretical analysis remains incomplete. In practice, due to imperfect detection efficiency $\eta < 1$, there are undetected events denoted as u. If one discards these undetected events, it will result in a severe *detection loophole*. Here, to test local realism with Hardy's paradox without *detection loophole*, we take these undetected events u into account. During each trial, Alice and Bob choose one of two measurement settings, respectively. The measurement results for Alice and Bob are denoted as ternary elements $a, b \in \{0, 1, u\}$, respectively. Inspired by Refs. [54,55], when Hardy's conditions $P(00|A_2B_2) = 0$, $P(01|A_1B_2) = 0$, and $P(10|A_2B_1) = 0$ are satisfied, there must be Hardy's value $P_{\text{Hardy}} = P(00|A_1B_1) - P(0u|A_1B_2) - P(u0|A_2B_1) \leq 0$ for local hidden variable models. However, positive Hardy's values can be achieved for quantum theory with

$$P_{\text{Hardy}}^{\max}(\eta) = \frac{1}{2}[1 - \sqrt{1 + 4\eta(3\eta - 2)}] + 3\eta[1 - 3\eta + \sqrt{1 + 4\eta(3\eta - 2)}], \quad (1)$$

for $\eta \in (2/3, 1]$ (see Supplemental Material [56], Sec. I, for details).

In addition to the imperfect detection efficiency, due to the dark counts of detectors and multiple pairs of photons from the entangled source, there are also some double-click events in practical experiments, which correspond to cases where both result 1 and 0 are obtained simultaneously in a single laboratory. Here, to close the *detection loophole*, we designate these double-click events as inconclusive events u, too. Moreover, due to such imperfections, zero Hardy's conditions are experimentally unattainable. Consequently, a form of Hardy constrained Eberhard inequality $P_{\text{Hardy}} \leq 0$ together with three Hardy's conditions is necessary for a loophole-free Hardy's paradox test. Inspired by the strategy of tackling nonzero Hardy's conditions in Refs. [57,58], when Hardy's conditions $P(00|A_2B_2) = \varepsilon_1$, $P(01|A_1B_2) = \varepsilon_2$, and $P(10|A_2B_1) = \varepsilon_3$ are satisfied, there must be Hardy's value

$$P_{\text{Hardy}} = P(00|A_1B_1) - P(0u|A_1B_2) - P(u0|A_2B_1) - \sum_{i=1}^{3} \varepsilon_i \leq 0, \quad (2)$$

for LHV models. Here, u denotes inconclusive events including undetected events and double-click events, ε_i with $i \in \{1, 2, 3\}$ are small values for nonzero Hardy's conditions.

Another obstacle is that, compared with Bell inequality tests, the loophole-free Hardy's paradox test requires even higher detection efficiency and higher fidelity of the entangled states. For example, with the system detection efficiency ($\eta \approx 78.8\%$) and quantum state fidelity ($F \approx 98.66\%$) in Ref. [11], we show that the Hardy's value should be less than 10^{-6}, which is very difficult to realize in a loophole-free manner (see Supplemental Material, Sec. I, for detail). In the following sections, we experimentally demonstrate a loophole-free Hardy constrained Eberhard inequality violation by quantum mechanics statistics as a paradox against local realistic theories.

Experiments—The present Hardy's paradox test is illustrated in Fig. 1. Using a pump laser of 780 nm, the polarization-entangled 1560 nm photon pairs are generated through spontaneous down conversion (SPDC) in the PPKTP crystal within a Sagnac loop. Then the two photons of a pair are transmitted to Alice's and Bob's laboratories through fiber links for measurements. To close the *locality loophole* and address the *freedom-of-choice loophole* [8–10], we design a space-time configuration for our system, as shown in Fig. 2. Specifically, it is necessary to spacelike separate the setting choices on one side (the first dots on the red bar and blue bar denote the beginning of setting choice) from the measurements output on the other side (the last dots on the two bars denote the end of the measurement), as well as from the emission of the pump photons (the coordinate origin denotes the beginning of the emission of photons, and the second dots on the two bars denote the

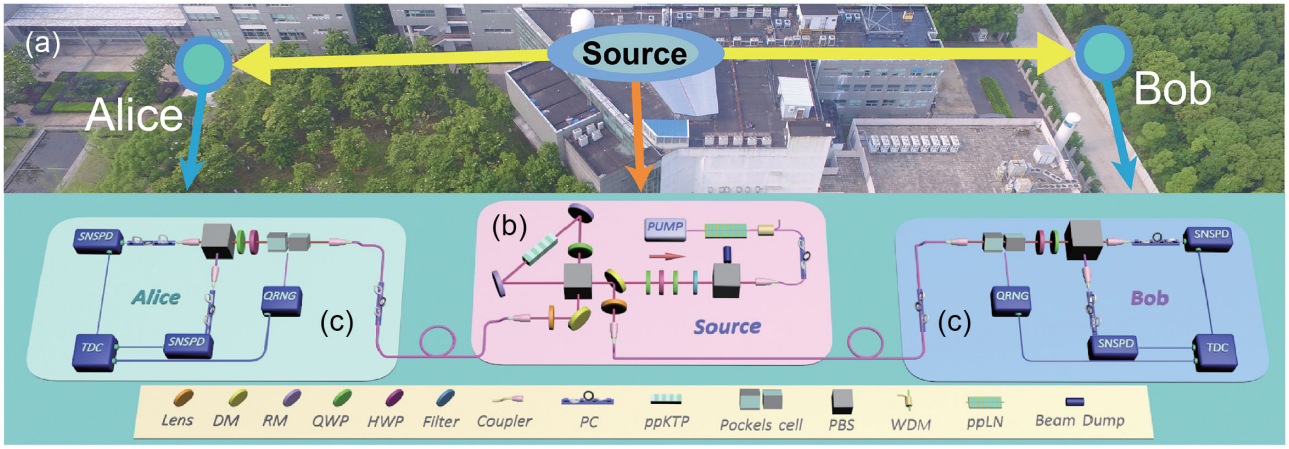

FIG. 1. Schematics of the experiment for the loophole-free Hardy's paradox. (a) Bird's-eye view of the experimental apparatus: Alice and Bob are located on opposite sides of the entanglement source, and the straight-line distance between Alice (Bob) and the source is $93 \pm 1 (90 \pm 1)$ m. (b) Preparation of the entangled photon pairs: light pulses with a duration of 10 ns and a repetition rate of 200 kHz, generated by a 1560 nm seed laser diode (LD), undergo amplification through an erbium-doped fiber amplifier (EDFA). Subsequently, the pulses are frequency-doubled using an in-line periodically poled lithium niobate (PPLN) crystal. The remaining 1560 nm light is eliminated by a wavelength-division multiplexor (WDM) and spectral filters. Two 780 nm quarter-wave plates (QWPS) and a half-wave plate (HWP) before the Sagnac loop are used to control the polarization of the pump laser, thereby changing the relative amplitude and phase of the created polarization-entangled photon state.Then the 780 nm pump photons are fed into the periodically poled potassium titanyl phosphate (PPKTP) crystal in the Sagnac loop, consisting of two reflection mirrors (RMs) and a dual-wavelength polarizing beam splitter (PBS), to generate polarization-entangled photon pairs of 1560 nm. After the Sagnac loop, dichroic mirrors (DM) are used to remove the residual 780 nm pump laser. Then the entangled photons are collected into optical fibers by couplers and transferred to Alice and Bob at opposite sites for polarization projection and measurements. (c) Single-photon polarization measurement: on the measurement side, the photons pass through the fiber and then undergo polarization state measurements. The setup for performing single-photon polarization measurements consists of a Pockels cell, QWP, HWP, and PBS. And the photons are finally collected into a single-mode optical fiber for detection by superconducting nanowire single-photon detectors (SNSPDs). There are two SNSPDs at each side to collect the photons transmitted and reflected at the PBS. The measurement settings choice is performed under a quantum random number generator (QRNG), which is triggered by a 200 kHz signal and generates a random output with a 1:1 ratio of 0 and 1. Here, 0 corresponds to a low voltage and 1 corresponds to a high voltage. After the random signal is generated, it is applied to the Pockels cell, which modifies the polarization measurement by exerting different influences on the polarization at different voltage levels. The time-digital convertor (TDC) is applied to keep track of the photon detection and random number generation events.

end of setting choice), which can also be viewed as the emission of the hidden variable λ. The synchronization of the experimental system is achieved by locking the seed laser for the pump light, the QRNG for the setting choice, and the time-digital convertor (TDC) for the signal collection to the same clock. We carefully adjust the relative delay between the QRNG and pump light to ensure that the polarization of the photons can be modulated when the setting choice signal is simultaneously applied to the Pockels cell. Meanwhile, Alice's measurement station is separated far apart from Bob's measurement station (93 m for Alice from the source to her laboratory, and 90 m for Bob's case), and the lengths of the optical fibers (129 m for Alice and 116 m for Bob) are set appropriately to ensure time delays of 627 ns and 563 ns, respectively, from photon generation to detection.

Furthermore, concerning the *freedom-of-choice loophole*, we need to make sure that the random numbers used for measurement setting choices are completely undisturbed and truly random, i.e., the local hidden variables cannot manipulate the generation of random numbers. In principle, because there is an overlap between the backward light cones of two QRNGs and the pump laser, the independence and randomness of Alice's and Bob's random numbers cannot be confirmed without making any assumptions [9]. Here, the high-speed QRNGs we used can generate random numbers within a time interval of 100 ns after receiving the trigger signal, and the delay time can be flexibly adjusted to accommodate our space-time configuration. Thus the freedom-of-choice loophole can be addressed by assuming that the random numbers from QRNG are truly independent from any local hidden variables.

The measurements of Alice and Bob consist of Pockels cells, HWPs, PBSs in turn and finally SNSPDs. To distinguish the results 0, 1, and u experimentally, we place two detectors on the two output ports of the PBS and label the clicks on the transmission and reflection paths as 0 and 1, respectively. In addition, we denote the undetected events (absence of detector clicks) and double-click events (i.e., clicks on both detectors at one station) as u. The system heralding efficiencies are measured to be $82.1\% \pm 0.2\%$ ($82.4\% \pm 0.2\%$) for the transmission (reflection) path

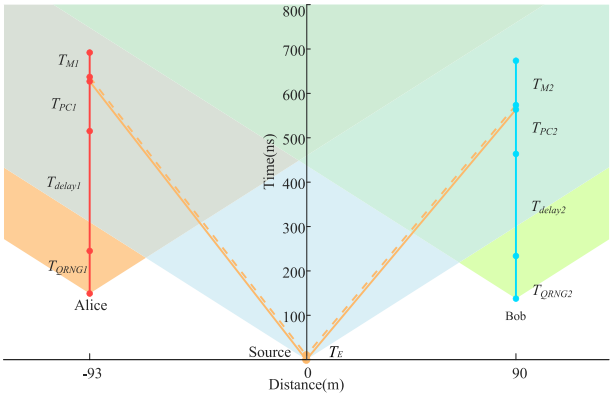

FIG. 2. Space-time diagram for the experimental events. The red (blue) bar and dots represent the crucial times and nodes for Alice's (Bob's) measurement. The coordinate origin denotes the beginning of the emission of the photon pairs. The orange line represents the space-time relationship of photon propagation in the optical fiber (the solid orange line is for the photons generated at the onset of generation, the dashed orange line is for the photons at the end of generation). $T_{\mathrm{E}} = 10$ ns is the duration required to generate entangled photon pairs. $T_{\mathrm{QRNG}\,1,2}$ is the duration for QRNG to generate random bits to control the Pockels cells. $T_{\mathrm{delay}\,1,2}$ is the time required between the random bits' generation and transferred to Pockels cells. $T_{\mathrm{PC}\,1,2}$ is the preparation time for the Pockels cells to be ready for the projection measurements after obtaining random bits from QRNGs. $T_{\mathrm{M}\,1,2}$ is the duration for SNSPDs to output electric signals. $T_{\mathrm{QRNG}\,1} = T_{\mathrm{QRNG}\,2} = 96$ ns, $T_{\mathrm{delay}\,1} = 270$ ns, $T_{\mathrm{delay}\,2} = 230$ ns, $T_{\mathrm{PC}\,1} = 112$ ns, $T_{\mathrm{PC}\,2} = 100$ ns, $T_{\mathrm{M}\,1} = 55$ ns, $T_{\mathrm{M}\,2} = 100$ ns. The linear distance between Alice (Bob) and the source is $93 \pm 1 (90 \pm 1)$ m, and the corresponding fiber length is 129 (116) m.

for Alice, and $82.1\% \pm 0.2\%$ ($82.2\% \pm 0.2\%$) for the transmission (reflection) path for Bob, using SNSPDs with efficiencies higher than 96%. The heralding efficiencies are determined by the ratio of twofold coincidence events to single counts, corresponding to the total events detected by a single detector directly measured across the entire system without accounting for any losses. These efficiencies significantly surpass the recorded values in previous loophole-free Bell tests with photons (see Table I). Furthermore, because the efficiency of SNSPD is polarization sensitive, we place a PC closely before each SNSPD. We utilize these PCs to adjust the efficiencies of the two paths at each measurement site to be close, since any discrepancy in efficiencies can be interpreted as a change of the measurement bases (because this offset affects the ratio of the probabilities of detecting photons in the transmission and reflection paths). And we employ the Hardy constrained Eberhard inequality of the form Eq. (2), which considers all detection events and inherently closes this loophole.

To observe Hardy's nonlocality in this experiment, the quantum state $|\psi(\theta)\rangle = \cos(\theta)|HV\rangle + \sin(\theta)|VH\rangle$ and measurement settings $A_i = \cos(\theta_{A_i})\sigma_z + \sin(\theta_{A_i})\sigma_x$, $B_j = \cos(\theta_{B_j})\sigma_z + \sin(\theta_{B_j})\sigma_x$, where $i, j \in 1, 2$ are

TABLE I. Efficiencies and fidelity in the existing photonic experiments of loophole-free Bell tests and related applications. The efficiencies are averaged over Alice's and Bob's detection efficiency.

Label	Experiment	Year	Type	Efficiency	Fidelity
(1)	Shalm *et al.* [9]	2015	Bell test	75.15%	
(2)	Giustina *et al.* [10]	2015	Bell test	77.40%	
(3)	Bierhorst *et al.* [22]	2018	QRNG	75.50%	
(4)	Liu *et al.* [23]	2018	QRNG	78.65%	
(5)	Li *et al.* [11]	2018	Bell test	78.75%	98.66%
(6)	Zhang *et al.* [24]	2020	QRNG	76.00%	
(7)	Shalm *et al.* [25]	2021	QRNG	76.30%	
(8)	Li *et al.* [26]	2021	QRNG	81.35%	
(9)	This work	2023	Hardy test	82.22%	99.10%

preoptimized for the overall efficiency $\eta_A(\eta_B)$. Specifically, in the optimization, we set the detection efficiency to be $\eta = 82\%$, the corresponding quantum state, Alice's and Bob's measurement settings are optimized to be $\theta = 0.2764$, $\{\theta_{A_1} = -2.8417, \theta_{A_2} = 2.1628\}$ and $\{\theta_{B_1} = 0.2999, \theta_{B_2} = -0.9788\}$ in radian, respectively (see Supplemental Material, Sec. I for details). In the implementation, we measure the visibility to be 99.5% and 98.4% in horizontal and vertical basis and diagonal and antidiagonal basis, respectively. Furthermore, we characterize the quantum state by state tomography measurement, and the fidelity of the nonmaximally polarization-entangled state is 99.10% (see Supplemental Material, Sec. II, for more details). To reduce the dark count, both windows in which Alice and Bob record detection events are set to 15 ns, which are centered on the expected arrival time of Alice's and Bob's photons. The average dark count in this

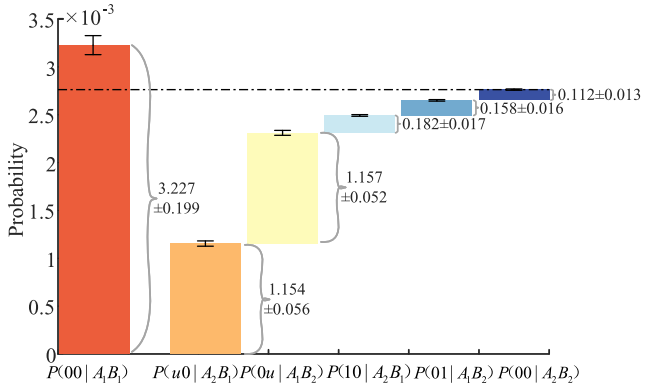

FIG. 3. Bar chart of the six joint probabilities for the present Hardy's paradox. The height of each bar shows the value of the corresponding joint probability. The last three bars represent the three Hardy's conditions, which are small quantities relative to the other probabilities. The height of the first bar, representing $P(00|A_1B_1)$, is greater than the sum of the other five bars, indicating a positive P_{Hardy}. These results present strong evidence against local realism.

window is less than 5 counts per second. After stable execution of 6 h with 4.32×10^9 trials, as shown in Fig. 3, the observed probabilities in the Hardy's paradox test are $\varepsilon_1 = P(00|A_2B_2) = (1.120 \pm 0.136) \times 10^{-4}$, $\varepsilon_2 = P(01|A_1B_2) = (1.578 \pm 0.162) \times 10^{-4}$, $\varepsilon_3 = P(10|A_2B_1) = (1.818 \pm 0.171) \times 10^{-4}$, $P(0u|A_1B_2) = (1.157 \pm 0.052) \times 10^{-3}$, $P(u0|A_2B_1) = (1.154 \pm 0.056) \times 10^{-3}$, and $P(00|A_1B_1) = (3.227 \pm 0.199) \times 10^{-3}$. These probabilities result in a positive Hardy's value $P_{\text{Hardy}} = 4.646 \times 10^{-4}$ based on the Eq. (2), which is more than 5 standard deviations according to the observed statistics (here the standard deviation is $\sigma = 7.771 \times 10^{-5}$).

To quantify the statistical significance of Hardy's violation, we conduct a hypothesis test of local realism with the prediction-based-ratio (PBR) method of analysis, which allows to analyze the experimental results without assuming independent and identical conditions [53]. The null hypothesis is that the experimental results can be accounted for by local hidden variable models. The maximal probability that the observed experimental results comply with the null hypothesis is quantified by a statistical p value. Under the PBR analysis, our demonstration shows that the p value is upper-bounded by 10^{-16348}, providing extremely strong evidence against local realism (see Supplemental Material, Sec. III for more details) [56].

Discussion and conclusion—We have presented a refinement of the theoretical analysis of loophole-free demonstration of Hardy's paradox. By applying high detection efficiency, a high fidelity entangled photon source, fast QRNGs, and spacelike separating the events corresponding to measurement setting choices, entangled state preparations and photon detections, we have simultaneously closed the *locality loophole*, and addressed the *freedom-of-choice loophole* in the experiment. By combining the strategy of treating double-click events as inconclusive events and considering local hidden variable models under imperfect detection efficiencies, we have also closed the *detection loophole*.

After stable execution for 6 h, a positive Hardy's value $P_{\text{Hardy}} = 4.646 \times 10^{-4}$ is observed, exceeding 5 standard deviations. Based on a null hypothesis test, the p value that the possibility our results can be explained by local realistic theories does not exceed 10^{-16348}. Therefore, our experiment provides a significant evidence that quantum mechanical description of physical quantities cannot be accounted for by local realism. Besides this fundamental interest, these results mark a milestone for quantum information applications based on the Hardy's paradox.

Acknowledgments—This work has been supported by the National Natural Science Foundation of China (Grants No. T2125010, No. 62375252, and No. 62031024), the Shanghai Municipal Science and Technology Major Project (Grants No. 2019SHZDZX01), the Anhui Initiative in Quantum Information Technologies (Grant No. AHY010300), the Innovation Program for Quantum Science and Technology (Grants No. 2021ZD0300800, No. 2021ZD0301100), as well as the National Key R&D Program of China (Grant No. 2019YFA0308700). J. L. C. has been supported by the National Natural Science Foundations of China (Grants No. 12275136 and No. 12075001) and the 111 project of B23045. S. Z. has been supported by the Research Startup Foundation of Hangzhou Dianzi University (No. KYS275623071) and Zhejiang Provincial Natural Science Foundation of China under Grant No. LQ24A050005.

S.-R. Z., S. Z., and H.-H. D. contributed equally to this letter.

[1] A. Einstein, B. Podolsky, and N. Rosen, Phys. Rev. **47**, 777 (1935).
[2] J. S. Bell, Physics **1**, 195 (1964).
[3] J. F. Clauser, M. A. Horne, A. Shimony, and R. A. Holt, Phys. Rev. Lett. **23**, 880 (1969).
[4] P. Holland, Found. Phys. **35**, 177 (2005).
[5] N. Brunner, D. Cavalcanti, S. Pironio, V. Scarani, and S. Wehner, Rev. Mod. Phys. **86**, 419 (2014).
[6] S. J. Freedman and J. F. Clauser, Phys. Rev. Lett. **28**, 938 (1972).
[7] A. Aspect, P. Grangier, and G. Roger, Phys. Rev. Lett. **49**, 91 (1982).
[8] B. Hensen, H. Bernien, A. E. Dréau, A. Reiserer, N. Kalb, M. S. Blok, J. Ruitenberg, R. F. Vermeulen, R. N. Schouten, C. Abellán *et al.*, Nature (London) **526**, 682 (2015).
[9] L. K. Shalm, E. Meyer-Scott, B. G. Christensen, P. Bierhorst, M. A. Wayne, M. J. Stevens, T. Gerrits, S. Glancy, D. R. Hamel, M. S. Allman *et al.*, Phys. Rev. Lett. **115**, 250402 (2015).
[10] M. Giustina, M. A. M. Versteegh, S. Wengerowsky, J. Handsteiner, A. Hochrainer, K. Phelan, F. Steinlechner, J. Kofler, J.-A. Larsson, C. Abellán *et al.*, Phys. Rev. Lett. **115**, 250401 (2015).
[11] M.-H. Li, C. Wu, Y. Zhang, W.-Z. Liu, B. Bai, Y. Liu, W. Zhang, Q. Zhao, H. Li, Z. Wang *et al.*, Phys. Rev. Lett. **121**, 080404 (2018).
[12] D. Rauch, J. Handsteiner, A. Hochrainer, J. Gallicchio, A. S. Friedman, C. Leung, B. Liu, L. Bulla, S. Ecker, F. Steinlechner *et al.*, Phys. Rev. Lett. **121**, 080403 (2018).
[13] S. Storz, J. Schär, A. Kulikov, P. Magnard, P. Kurpiers, J. Lütolf, T. Walter, A. Copetudo, K. Reuer, A. Akin *et al.*, Nature (London) **617**, 265 (2023).
[14] W. Rosenfeld, D. Burchardt, R. Garthoff, K. Redeker, N. Ortegel, M. Rau, and H. Weinfurter, Phys. Rev. Lett. **119**, 010402 (2017).
[15] D. Mayers and A. Yao, in *Proceedings 39th Annual Symposium on Foundations of Computer Science (Cat. No. 98CB36280)* (IEEE, New York, 1998), pp. 503–509.
[16] J. Barrett, L. Hardy, and A. Kent, Phys. Rev. Lett. **95**, 010503 (2005).
[17] A. Acín, N. Gisin, and L. Masanes, Phys. Rev. Lett. **97**, 120405 (2006).

[18] A. Acín, N. Brunner, N. Gisin, S. Massar, S. Pironio, and V. Scarani, Phys. Rev. Lett. **98**, 230501 (2007).
[19] R. Colbeck, Ph.D. thesis, University of Cambridge, 2007.
[20] S. Pironio, A. Acín, S. Massar, A. B. de La Giroday, D. N. Matsukevich, P. Maunz, S. Olmschenk, D. Hayes, L. Luo, T. A. Manning *et al.*, Nature (London) **464**, 1021 (2010).
[21] R. Colbeck and R. Renner, Nat. Phys. **8**, 450 (2012).
[22] P. Bierhorst, E. Knill, S. Glancy, Y. Zhang, A. Mink, S. Jordan, A. Rommal, Y.-K. Liu, B. Christensen, S. W. Nam *et al.*, Nature (London) **556**, 223 (2018).
[23] Y. Liu, Q. Zhao, M.-H. Li, J.-Y. Guan, Y. Zhang, B. Bai, W. Zhang, W.-Z. Liu, C. Wu, X. Yuan *et al.*, Nature (London) **562**, 548 (2018).
[24] Y. Zhang, L. K. Shalm, J. C. Bienfang, M. J. Stevens, M. D. Mazurek, S. W. Nam, C. Abellán, W. Amaya, M. W. Mitchell, H. Fu *et al.*, Phys. Rev. Lett. **124**, 010505 (2020).
[25] L. K. Shalm, Y. Zhang, J. C. Bienfang, C. Schlager, M. J. Stevens, M. D. Mazurek, C. Abellán, W. Amaya, M. W. Mitchell, M. A. Alhejji *et al.*, Nat. Phys. **17**, 452 (2021).
[26] M.-H. Li, X. Zhang, W.-Z. Liu, S.-R. Zhao, B. Bai, Y. Liu, Q. Zhao, Y. Peng, J. Zhang, Y. Zhang *et al.*, Phys. Rev. Lett. **126**, 050503 (2021).
[27] W.-Z. Liu, Y.-Z. Zhang, Y.-Z. Zhen, M.-H. Li, Y. Liu, J. Fan, F. Xu, Q. Zhang, and J.-W. Pan, Phys. Rev. Lett. **129**, 050502 (2022).
[28] F. Xu, Y.-Z. Zhang, Q. Zhang, and J.-W. Pan, Phys. Rev. Lett. **128**, 110506 (2022).
[29] D. P. Nadlinger, P. Drmota, B. C. Nichol, G. Araneda, D. Main, R. Srinivas, D. M. Lucas, C. J. Ballance, K. Ivanov, E.-Z. Tan *et al.*, Nature (London) **607**, 682 (2022).
[30] W. Zhang, T. van Leent, K. Redeker, R. Garthoff, R. Schwonnek, F. Fertig, S. Eppelt, W. Rosenfeld, V. Scarani, C. C.-W. Lim *et al.*, Nature (London) **607**, 687 (2022).
[31] C.-L. Li, K.-Y. Zhang, X. Zhang, K.-X. Yang, Y. Han, S.-Y. Cheng, H. Cui, W.-Z. Liu, M.-H. Li, Y. Liu *et al.*, Proc. Natl. Acad. Sci. U.S.A. **120**, e2205463120 (2023).
[32] V. Zapatero, T. van Leent, R. Arnon-Friedman, W.-Z. Liu, Q. Zhang, H. Weinfurter, and M. Curty, npj Quantum Inf. **9**, 10 (2023).
[33] I. Šupić, J. Bowles, M.-O. Renou, A. Acín, and M. J. Hoban, Nat. Phys. **19**, 670 (2023).
[34] W.-Z. Liu, M.-H. Li, S. Ragy, S.-R. Zhao, B. Bai, Y. Liu, P. J. Brown, J. Zhang, R. Colbeck, J. Fan *et al.*, Nat. Phys. **17**, 448 (2021).
[35] D. M. Greenberger, M. A. Horne, and A. Zeilinger, in *Bell's Theorem, Quantum Theory and Conceptions of the Universe*, edited by M. Kafatos (Springer Netherlands, Dordrecht, 1989), pp. 69–72.
[36] D. M. Greenberger, M. A. Horne, A. Shimony, and A. Zeilinger, Am. J. Phys. **58**, 1131 (1990).
[37] L. Hardy, Phys. Rev. Lett. **71**, 1665 (1993).
[38] N. D. Mermin, Am. J. Phys. **62**, 880 (1994).
[39] A. Mukherjee, A. Roy, S. S. Bhattacharya, S. Das, M. R. Gazi, and M. Banik, Phys. Rev. A **92**, 022302 (2015).
[40] H.-W. Li, M. Pawłowski, R. Rahaman, G.-C. Guo, and Z.-F. Han, Phys. Rev. A **92**, 022327 (2015).
[41] R. Rahaman, M. G. Parker, P. Mironowicz, and M. Pawłowski, Phys. Rev. A **92**, 062304 (2015).
[42] R. Ramanathan, M. Horodecki, H. Anwer, S. Pironio, K. Horodecki, M. Grünfeld, S. Muhammad, M. Bourennane, and P. Horodecki, arXiv:1810.11648.
[43] A. Rai, M. Pivoluska, S. Sasmal, M. Banik, S. Ghosh, and M. Plesch, Phys. Rev. A **105**, 052227 (2022).
[44] S. Zhao, R. Ramanathan, Y. Liu, and P. Horodecki, Quantum **7**, 1114 (2023).
[45] D. Boschi, S. Branca, F. De Martini, and L. Hardy, Phys. Rev. Lett. **79**, 2755 (1997).
[46] M. Barbieri, F. De Martini, G. Di Nepi, and P. Mataloni, Phys. Lett. A **334**, 23 (2005).
[47] G. Vallone, I. Gianani, E. B. Inostroza, C. Saavedra, G. Lima, A. Cabello, and P. Mataloni, Phys. Rev. A **83**, 042105 (2011).
[48] L. Chen and J. Romero, Opt. Express **20**, 21687 (2012).
[49] E. Karimi, F. Cardano, M. Maffei, C. de Lisio, L. Marrucci, R. W. Boyd, and E. Santamato, Phys. Rev. A **89**, 032122 (2014).
[50] L. Chen, W. Zhang, Z. Wu, J. Wang, R. Fickler, and E. Karimi, Phys. Rev. A **96**, 022115 (2017).
[51] M. Yang, H.-X. Meng, J. Zhou, Z.-P. Xu, Y. Xiao, K. Sun, J.-L. Chen, J.-S. Xu, C.-F. Li, and G.-C. Guo, Phys. Rev. A **99**, 032103 (2019).
[52] S. Das and G. Paul, ACM Trans. Quantum Comput. **1**, 1 (2020).
[53] Y. Zhang, S. Glancy, and E. Knill, Phys. Rev. A **84**, 062118 (2011).
[54] P. H. Eberhard, Phys. Rev. A **47**, R747 (1993).
[55] W. Y. Hwang, I. G. Koh, and Y. D. Han, Phys. Lett. A **212**, 309 (1996).
[56] See Supplemental Material at http://link.aps.org/supplemental/10.1103/PhysRevLett.133.060201, which includes Refs. [11,37,53–55,57–59], for additional information about the experimental methods and theoretical simulations.
[57] G. C. Ghirardi and L. Marinatto, Phys. Rev. A **74**, 062107 (2006).
[58] D. Braun and M.-S. Choi, Phys. Rev. A **78**, 032114 (2008).
[59] S. Kullback and R. A. Leibler, Ann. Math. Stat. **22**, 79 (1951).